The effects of particle-induced oxidative damage from exposure to airborne fine particulate matter components in the vicinity of landfill sites on Hong Kong

K. H. Lui[1,10], Tim P. Jones[2], Kelly BéruBé[3], Steven Sai Hang Ho[4], S.H.L.Yim[5,6], Jun-Ji Cao[4,7], S. C. Lee[8], Linwei Tian[9], Dae Wi Min[10], K. F. Ho[1*]

[1] *The Jockey Club School of Public Health and Primary Care, The Chinese University of Hong Kong, Hong Kong, China*

[2] *School of Earth and Ocean Sciences, Cardiff University, Park Place, Cardiff, U.K.*

[3] *School of Biosciences, Cardiff University, Museum Avenue, Cardiff, U.K.*

[4] *Key Division of Atmospheric Sciences, Desert Research Institute, Reno, NV 89512, U.S.A.*

[5] *Department of Geography and Resource Management, The Chinese University of Hong Kong, Hong Kong, China*

[6] *Stanley Ho Big Data Decision Analytics Research Centre, The Chinese University of Hong Kong, Shatin, N.T., Hong Kong, China*

[7] *Institute of Global Environmental Change, Xi'an Jiaotong University, Xi'an, China*

[8] *Department of Civil and Structural Engineering, Research Center of Urban Environmental Technology and Management, The Hong Kong Polytechnic University, Hong Kong, China*

[9] *School of Public Health, The University of Hong Kong, Hong Kong, China*

[10] *Division of Environmental Science and Engineering, Pohang University of Science and Technology (POSTECH), Pohang 37673, Korea*

[*]Corresponding author. Tel.: +852 22528763; fax: +852 26063500

E-mail address: kfho@cuhk.edu.hk

Abstract

The physical, chemical and bioreactivity characteristics of fine particulate matter ($PM_{2.5}$) collected near (< 1km) two landfill sites and downwind urban sites were investigated. The $PM_{2.5}$ concentrations were significantly higher in winter than summer. Diurnal variations of $PM_{2.5}$ were recorded at both landfill sites. Soot aggregate particles were identified near the landfill sites, which indicated that combustion pollution due to landfill activities was a significant source. High correlation coefficients (*r*) implied several inorganic elements and water-soluble inorganic ions (vanadium (V), copper (Cu), chloride (Cl^-), nitrate (NO_3^-), sodium (Na) and potassium (K)) were positively associated with wind flow from the landfill sites. Nevertheless, no significant correlations were also identified between these components against DNA damage. Significant associations were observed between DNA damage and some heavy metals such as cadmium (Cd) and lead (Pb), and total Polycyclic Aromatic Hydrocarbons (PAHs) during the summer. The insignificant associations of DNA damage under increased wind frequency from landfills suggested that the $PM_{2.5}$ loading from sources such as regional sources was possibly an important contributing factor for DNA damage. This outcome warrants the further development of effective and source-specific landfill management regulations for particulate matter production control to the city.

Keywords:

Landfills; $PM_{2.5}$; Ambient air; Landfill composites; Oxidative potential

1. **Introduction**

Landfill has been traditionally regarded as a common method of organized waste disposal and is a widely used waste management practice around the world. According to the Hong Kong Environmental Protection Department, the disposal of total solid waste at landfills averages 15,102 tonnes per day, with 10,159 tonnes per day classified as municipal solid waste (MSW) (e.g. domestic waste, commercial waste and industrial waste). The average disposal rate of MSW in Hong Kong was approximately 1.4 kg per capita daily (HKEPD, 2015), compared to approximately 2.0 kg per capita daily in the United States (U.S. EPA, 2013). The problem of waste disposal is considered as one of the most serious environmental issues in Hong Kong. Operating landfills can generate a variety of air pollutants such as particulate matter (PM) and the emitted particulates can contain inorganic and organic components (Koshy et al., 2009; Macklin et al., 2011). A study by Deed (2004) showed a large proportion of the inorganic components in PM collected at landfills are mineral-based and derived from wind-blown soil. Typical hazardous particles generated at landfills are toxic crystalline silica and needle-like metal particles that are generated by waste fragmentisers.

Airborne PM is a health concern worldwide due to adverse health effects. A previous epidemiological study demonstrated exposure to PM could intensify respiratory morbidity and mortality (Pope III et al., 1995). Oxidative stress is a mechanism by which exposure to PM can potentially cause adverse health effects when overproduction of oxidants (e.g., Reactive Oxygen Species (ROS) and free radicals) offsets anti-oxidative defences (Charrier et al., 2014). Fine particulate matter (aerodynamic diameter < 2.5 μm: $PM_{2.5}$) can elicit adverse inflammatory responses by depositing in the lung periphery (Bitterle et al., 2006). The plasmid scission assay (PSA) is an established technique for assessing the oxidative capacity (ROS) (Gilmour et al., 1994; Stone et al., 1998; Moreno et al., 2004; Lingard et al., 2005; Miller et al., 2012). Previous studies have applied this technique to understand the toxicity of atmospheric particulates (Koshy et al., 2007; Koshy et al., 2009; Shao et al., 2013; Xiao et al., 2014). The components such as elemental carbon (EC) and organic carbon (OC) can constitute a significant proportion of $PM_{2.5}$ (20-80%) (Rogge et al., 1993; Sillanpää et al., 2005). The water-soluble fractions of atmospheric aerosol contains components (e.g. ions) that capable to increase the solubility of toxic organic compounds (e.g. polycyclic aromatic hydrocarbons: PAHs) and further to increase toxicity to human health (Wang et al., 2003).The bioavailable transition metals on the particle surfaces can also promote free radicals generation and lead to oxidative damage (Costa and Dreher, 1997; Donaldson et al., 1996).

Several studies have revealed the health risks posed by landfill sites (such as cancer or congenital anomalies) (Jarup et al., 2012; Palmer et al., 2005), but there is insufficient investigations about the bioactivity of $PM_{2.5}$ from municipal landfill sites in Hong Kong. The aims of this study are to: 1) To investigate the physicochemical characteristics of $PM_{2.5}$ samples collected from locations near (< 1km) MSW landfill sites; 2) To determine the oxidative stress of $PM_{2.5}$ samples using the generation of reactive oxygen species (ROS); 3) To determine the relationship between physical and chemical characteristics of $PM_{2.5}$ and their bioreactivity collected near (< 1km) the landfill sites and in the downwind urban sites.

2. Materials and methods

2.1 Sampling locations

Five sampling sites were selected for this study (Figure 1). Two sites were located adjacent to the landfill areas (with both <500 m from the landfill sites) namely West New Territories (WENT) and South East New Territories (SENT). The WENT landfill has an area of 110 ha with waste intake ~ 7,500 tonnes per day (HKEPD, 2015). The sampling site of WENT was located at Ha Pak Nai, which was 100 m away from the WENT landfill. The SENT landfill has an area of 100 ha waste intake ~4,000 tonnes per day (HKEPD, 2015). The sampling site of SENT was located at Tseung Kwan O Industrial Estate approximately 300 m from the SENT landfill. Two urban sites were located in a mixture of residential and commercial areas namely as Tin Shui Wai (TSW) and Tseung Kwan O (TKO), which are the nearest local hubs to WENT and SENT landfill respectively. The SENT landfill was to receive only construction waste after January of 2016 to address the odour problem. The waste intake at the SENT Landfill was anticipated to be reduced to approximately 500 vehicular loads after the regulation amendment (HKEPD, 2016). Hok Tsui (HT) was selected as the rural site at the south-eastern tip of Hong Kong Island. The sampling site is in a remote area and far removed from any anthropogenic activities, ~2.5 km away from major traffic (Shek O Road). Details of sampling sites can be found in Figure S1-2 (Supplementary Material).

2.2 Experimental procedures

2.2.1 Sample collection

Details of the sample collection can be found in Text S1 (Supplementary Material).

2.3 Analytical methods

2.3.1 Field emission scanning electron microscope (FESEM) analysis

The FESEM analysis was used for particle imaging according to standard procedures (Jones et al., 2006). Particles on the Teflon filters were extracted with distilled deionized water, as this extractant was considered to be least chemically aggressive solution. This extraction was essential as the particles were embedded deep in the body of the filters and not seen on the filter surface. A consequence of this is that all water-soluble samples are lost in these analyses. The samples were then mounted on a conventional 12.5 mm aluminium stubs using Epoxy resin (Araldite™). Stubs were coated to improve imaging with evaporated gold–palladium

(Au–Pd 60: 40), using a Bio-Rad SC500 sputter coater under an inert argon atmosphere, to a thickness of 20 nm. A Veeco FEI Philips XL30 environmental SEM with a field emission gun was used for specimen imaging.

2.3.2 Chemical components analysis

Details of the chemical components (elements, water-soluble inorganic ions, organic carbon, elemental carbon and polycyclic aromatic hydrocarbons) analysis can be found in Text S2-5 (Supplementary Material). The abbreviation of individual chemical components can be referred to Table S2 (Supplementary Material).

2.3.3 Plasmid scission assay (PSA) for bioreactivity analysis

Details of the plasmid scission assay analysis can be found in Text S6 (Supplementary Material).

2.4 Statistical analysis

Statistical analysis was performed using SPSS 21.0 software. Details of the analysis can be found in Text S7. The significance level was set at $p < 0.05$.

3. Results and discussion

3.1 Diurnal variations of $PM_{2.5}$

The $PM_{2.5}$ mass concentrations acquired from real-time monitors have been cross-checked with filter-based concentration results to ensure performance optimization. Good correlations were observed between filter-based $PM_{2.5}$ mass concentrations and real time $PM_{2.5}$ mass concentrations at WENT and SENT in both seasons (Winter season: WENT: $r = 0.88$, $p < 0.01$, SENT: $r = 0.705$, $p < 0.01$; Summer season: WENT: $r = 0.89$, $p < 0.01$, SENT $r = 0.90$, $p <$

0.01). Figures 2 and 3 show temporal variations of hourly $PM_{2.5}$ level at WENT and SENT in winter and summer, respectively. Diurnal variations of $PM_{2.5}$ (Supplementary Materials: Figure S10) were observed in both landfill sites (especially in WENT). Pronounced diurnal variations of $PM_{2.5}$ concentrations were observed for WENT in both seasons. In WENT, $PM_{2.5}$ concentrations in winter were generally low from December to January, followed by reaching optimum in February. In summer, $PM_{2.5}$ concentrations were in general low from August to September and achieved maximum in early October. The $PM_{2.5}$ concentrations were subsequently decreased until November. In SENT, $PM_{2.5}$ concentrations reached minimum in January and increased in February. In summer, $PM_{2.5}$ concentrations were at minimum from July to August, followed by a peak observed in October. In addition, the $PM_{2.5}$ concentrations were significantly higher in winter than summer. In WENT high $PM_{2.5}$ levels were due to enhanced anthropogenic emissions with daytime activities (including landfill activities) in addition to local land–sea breeze circulations. In SENT high $PM_{2.5}$ levels were also observed during daytime, but the PM diurnal variations were different between seasons.

The contribution of $PM_{2.5}$ from different wind directions is illustrated by pollution roses in Figure S6 (Supplementary Material). The dominant wind directions at WENT was south/north in winter and south in summer. The $PM_{2.5}$ loadings were observed to increase under the dominant west and northwest surface winds and low wind speed in both seasons (Supplementary Materials: Figure S6: a and S6: c). The high PM2.5 loadings associated with low wind speed indicate the significant contribution of near sources. While the landfill is located at west of the sampling site, high $PM_{2.5}$ levels were potentially due to the influence of local activities that transferred from the landfill. However, more than 50% of surface winds were from the south or north in winter and south in summer from which low to high levels of $PM_{2.5}$ were also observed under these conditions. The dominant wind directions at SENT was east in winter and summer. The $PM_{2.5}$ loadings were observed to increase when surface winds were from the east (from landfill) and northwest (where the downtown area is around 4 km away from SENT) in winter (Supplementary Materials: Figure S6: b), which is consistent with the prevailing wind in winter in Hong Kong (Yim et al., 2009; Yim et al., 2010). The $PM_{2.5}$ levels at this site could possibly be due to local and regional PM sources in winter (Hou et al., 2018; Luo et al., 2018; Tong et al., 2018; Yim et al., 2019). In summer, no significant hotspots were identified after the analysis. The emission maps of respirable suspended particulate (RSP), nitrogen oxides and sulfur dioxide can be referred to Figure S7-9 (Supplementary Material).

Under real-time $PM_{2.5}$ monitoring, high $PM_{2.5}$ levels were observed in winter. The higher average $PM_{2.5}$ concentrations coupled with prevalent northerly to northeasterly winds were also observed during winter. This observation points to possibly a transfer of aged and contaminated air masses from the Pearl River Delta region to Hong Kong. The lower average $PM_{2.5}$ concentrations during the summer could be due to prevailing southerly or southeasterly winds drawing clean marine air masses from the South China Sea or the Northwest Pacific Ocean, diluting $PM_{2.5}$ concentrations (Wang et al., 2005; Yuan et al., 2006). In addition, heavy rainfall caused by the summer monsoon could remove ground-level $PM_{2.5}$ by wet deposition (Supplementary Materials: Table S1). During daytime under wind directions predominantly from landfills high $PM_{2.5}$ levels were observed, which suggested the $PM_{2.5}$ level could be affected by anthropogenic activities (locomotion, waste process, landfill surface dust, soot and mineral particles and vehicular exhaust) from the landfills.

A temporal pattern could be related to local meteorological factors. The local sea breeze was dominant (lower $PM_{2.5}$ concentration) from midnight until the early morning, while land breezes (higher $PM_{2.5}$ concentration) dominated in the remainder of the day. However, over 50% and 30% of surface winds were not from WENT and SENT landfills, respectively, and no significant association was observed between wind frequency from landfills and integrated

$PM_{2.5}$ mass concentrations. This implies $PM_{2.5}$ loading from other wind directions was an important contributing factor.

3.2 Particle morphology analysis

The airborne particles were classified into 3 types (soot aggregations, mineral matter and "other types") based on morphology and elemental compositions (Figure 4). Soot aggregates were commonly seen in the samples. For example several small soot particles were observed adhering to the surface of a non-crystalline (conchoidal fracture) glass particle (Figure 4: a-1). These composite particles contained C, O, Na, Al, Si and K element and the atomic percentages were 60.28%, 32.57%, 1.37%, 0.41%, 4.78%, and 0.58%, respectively. Other particles are seen as agglomerations of small spheres that predominantly consist of soot (Figure 4: a-2). The atomic percentages of C, O, Na, Al, Si, and K were 69.81%, 21.99%, 0.90%, 0.56%, 6.00%, and 0.74%, respectively. Numerous studies have confirmed that these soot aggregates possess the typical morphology of emissions from gasoline or diesel engines (Berube et al., 1999). These soot aggregate particles were collected near the landfill sites, which supports the view that gasoline/diesel combustion pollution (due to landfill activities) are a major component of landfill particulate pollution.

The identified mineral particles were derived from sources such as soil (used to cover the waste cells), resuspension of dust from unmade roadways, and other anthropogenic site activities (e.g. construction dust) (Yue et al., 2006). Mineral particles typically had irregular shapes with obvious crystalline structures rarely seen (Figure 4: b-1). The particles commonly consisted of an aggregation of mineral and soot particles. Some mineral grains were shown to possess a 'platy' morphology, an indication for clay minerals. The initial clay identification was further supported by the presence of Mg, Al, Si, K and Fe elements (atomic percentages of Mg, Al, Si, K and Fe were 0.36%, 1.67%, 10.13%, 1.24%, and 0.18%, respectively).

The origins of the particles in the 'other' category could not be confidentially identified from their morphology or elemental compositions; a common problem in some industry-sourced PM. Two examples are shown to illustrate the challenges presented when trying to identify the particle origins using analytical electron microscopy. These are the irregular shapes (Figure 4: c) and agglomerates type particles (Figure 4: d). The SEM-EDX analysis (Figure 4: c) revealed a large Fe component (atomic percentage = 5.74%), and the particle was interpreted as iron oxide (rust). The particles surrounding the Fe particles were predominately soot and platy (probably clay) mineral particles. The analysis (Figure 4: d) was shown to have high Si component (atomic percentage = 10.83%) with no visual indication of crystallinity, precluding common Si minerals. A number of micron to sub-micron size 'glass' particles agglomerated into a single particle is observed in the image. It is speculated that this could be a fragment of sintered glass where the smaller particles formed as an agglomerate under fusing temperature.

3.3 Ambient concentrations of chemical components in sampling locations

The samples collected by Teflon filters were used for mass concentration analysis. In winter, the highest average concentration of $PM_{2.5}$ was observed in WENT, whereas the SENT shows comparable $PM_{2.5}$ concentration range to the TKO site (Supplementary Materials: Table S3). Significant spatial variability of $PM_{2.5}$ levels were observed in WENT and TSW only in winter ($p < 0.05$). Significant differences between seasons were observed in WENT, SENT, TKO and HT sites ($p < 0.05$). Lower concentrations in summer could be due to enhanced thermal convection in the summer season, which is influenced by the Asian monsoon. The southwesterly summer monsoon could transfer clean oceanic aerosols from oceans (South China Sea and tropical Pacific Ocean) (Cao et al., 2004; Ho et al., 2003).

The OC and EC concentrations are shown in Table S4 (Supplementary Materials). Daily variation of OC and EC were observed at WENT and TSW, in addition to SENT and TKO all demonstrate similar trends (Supplementary Materials: Figure S11-12) and significant correlations between these two sites were observed in both seasons ($p < 0.05$). In contrast, significant spatial variability of OC and EC concentrations were only observed in WENT and TSW in winter ($p < 0.05$). The average concentrations of OC show significant differences between seasons in all sites ($p = 0.05$), whereas seasonal variability for EC was only observed in WENT and HT. The seasonal variations of OC could be due to prevailing north/northeast winds during winter that could transfer polluted/aged air masses from China. This condition could couple with stable atmospheric conditions in winter and resulted in the higher OC concentrations. The compositions of OC and EC in the $PM_{2.5}$ at all locations in winter are in a range of 17.2-29.1 and 4.4-5.0%, respectively. The contributions are lower in summer (3.9-15.0 and 2.2-8.8% for OC and EC, respectively). However, high OC-EC correlations ($r^2 > 0.75$) at all sampling sites in both seasons imply strong association between these two fractions and similar sources emissions.

The average concentrations of water-soluble inorganic ions are summarized in Table S5 (Supplementary Materials). The NO_3^-, SO_4^{2-} and NH_4^+ are the three most abundant ions in this study. The concentrations of these components further show statistically significantly different between seasons in all sampling locations, except for SO_4^{2-} in TSW ($p = 0.05$). Sulphate was the one of the major components in $PM_{2.5}$ which contributed in a range of 6.6-42.3 % in $PM_{2.5}$ mass in winter. The contributions were higher at all sampling locations in summer (22.9-60.8 %). The NO_3^- and NH_4^+ are also major constituents of atmospheric aerosols in Hong Kong with noticeable seasonal variations. Lower temperatures and less precipitation during winter favoured particulate NH_4NO_3 over HNO_3, and therefore higher NH_4NO_3 concentrations were observed in winter. Significant spatial variability of NO_3^-, SO_4^{2-} and NH_4^+ concentrations were observed in WENT and TSW only in winter (p = 0.05). High Na^+ concentrations observed in the stations could possibly be due to higher and persistent on-shore winds which generated abundant sea water droplets and marine aerosols. The higher Na^+ concentration in summer than winter could be potentially due to prevailing southerly or south-easterly winds in summer drawing marine air masses with large amount of sea salts bearing ions from the South China Sea or the Northwest Pacific Ocean.

The concentrations of elements are shown in Table S6 (Supplementary Materials). The average concentrations of total elements accounted for a range of 3.2-6.3% of $PM_{2.5}$ mass in winter; whereas in a range of 3.2-4.3% in summer. The average concentrations of total elements were minimum in summer and maximum in winter at all sampling locations, and a number of elements show significant differences between seasons, especially for crustal species (p = 0.05). However, vanadium (V), as a marker for oil combustion, shows distinct maximum in summer and minimum in winter in all locations. Residual oils are commonly used in diesel/ship engines which can produce significant amount of V emissions. Air flow over the ocean in summer could possibly explain the elevated V concentration from ship emissions in summer. Iron (Fe) is one of the major crustal elements in this study and the main source is from mineral dust. The average concentrations of Fe in HT (winter: 288.4 ng m^{-3}; summer: 83.8 ng m^{-3}) are lower than the other four sampling sites (winter: 432.2-582.8 ng m^{-3}; summer: 123.3-165.0 ng m^{-3}) in both seasons, this could possibly be due to the landfill and urban sampling sites having stronger influences by the mineral/road dust than background site (HT). The HT sampling station is in a remote area and far removed from any anthropogenic activities, ~2.5 km away from major traffic (Shek O Road). The observed concentrations suggest potential influences by the crustal matter in the four sampling stations, and the sites are considered to be in proximity to the local urban sources.

The concentrations of PAHs are shown in Table S7 (Supplementary Materials). The total PAHs concentration accounted for a range of 0.02-0.54% and 0.02-2.62 % in composition to the OC concentration in winter and summer, respectively. Statistically significant differences between seasons were observed in all sites (p = 0.05). The FLT, PHE, PYR, CHR and BbF were dominant components in all sampling locations which contributed ≥ 50% of the total PAHs. The United States Environmental Protection Agency (U.S. EPA) priority PAHs (Group B2 PAHs) in this study are in similar concentrations range to the Hong Kong roadside area, but lower than the concentrations in Guangzhou, Beijing and Xi'an (Leung et al., 2014; Zhang et al., 2016; Xu et al., 2016). According to the Chinese National Standard GB3095-2012, the maximum allowable 24 h average concentration for BaP is 2.5 ng m^{-3} (Zhang et al., 2016).The concentrations of BaP at all locations were below the threshold limit. The diagnostic ratios for PAHs were also determined and listed with other studies (Supplementary Materials: Figure S13). The ratios of INP/INP + BghiP and FLT/FLT + PYR from five sampling locations were in the range of 0.37-0.60 and 0.23-0.80, respectively. These ratios were consistent with a previous study and further suggested potential mixed influences from wood, coal and petroleum combustion (Okuda et al., 2010; Xu et al., 2016).

3.4 Oxidative potential - plasmid scission assay (PSA)

A positive dose-response relationship was identified between the amounts of DNA damage and sample concentrations, which indicates that higher mass concentrations of PM could cause higher oxidative potential. The TD_{50} and DNA damage (%) (100 μg ml^{-1} dosage) are listed in Table 1. The amount of damage to the plasmid DNA induced by $PM_{2.5}$ varied over the range of 24-92 % and 27-96 % in winter and summer, respectively. The WENT (and TSW) show the lowest average DNA damage (under 100 µg ml^{-1}) in winter. The oxidative potential of $PM_{2.5}$ samples in TKO was higher than other locations in winter. In contrast, both WENT and SENT show comparable DNA damage in summer. No samples demonstrated > 80% average DNA damage in TKO. This suggests samples collected near landfill in summer could contain higher oxidative capacity than in other locations. The DNA damage in summer was higher than winter in all locations (except TKO) and significant differences between seasons were observed in WENT, SENT, TSW and HT ($p < 0.05$). The results are consistent with a recent study in Beijing (Shao et al., 2017). Variation of DNA damage at WENT and TSW, together with SENT and TKO all showed significant correlations ($p < 0.05$) in summer.

3.5 Correlation analysis

3.5.1 Correlation between major chemical components

Correlation analysis was performed to identify associations between species. The influences of water-soluble inorganic ions and carbonaceous aerosol to $PM_{2.5}$ mass were confirmed by high correlations of $PM_{2.5}$ with OC, EC, ammonium, sulphate, and nitrate ($r > 0.7$, $p < 0.01$). Sulphates and nitrates are major inorganic ions and were well correlated with ammonium in all sites ($r > 0.5$, $p < 0.05$). The strong correlation between NH_4^+ and SO_4^{2-}, together with NH_4^+ and NO_3^- suggest that these ions primarily existed as ammonium sulphate ($(NH_4)_2SO_4$), ammonium bisulphate (NH_4HSO_4) and ammonium nitrate (NH_4NO_3) state.

Total PAHs was in good correlations with OC, EC and K^+ ($r > 0.5$, $p < 0.05$) and the highest correlation was observed between total PAHs with OC/nss-K^+ in WENT and SENT ($r >0.7$, $p <0.01$) in winter. Non-sea-salt potassium (nss-K^+) was used to exclude the influence of potassium derived from sea-salt and commonly used as source tracer for biomass burning activities. The results indicated regional impact from continental China was a determinant factor in winter. However, no significant association was observed between total PAHs and nss-K^+ in summer. Good correlations were observed between total PAHs and OC/EC, which indicated local combustion source (e.g. vehicular emission) was one of major sources for PAHs in summer. High Na^+ concentrations could be potentially due to sea water droplets and marine sources. The analysis showed Cl^- ions were correlated with Na^+ ions only in HT and SENT ($r > 0.5$, $p < 0.05$). Both locations are in proximity to sea with rich sea-salt particles. Nevertheless, reaction of nitric acid with sea-salt particles (NaCl) could generate sodium nitrate in the loss of chloride as product of gaseous hydrochloric acid (Zhuang et al., 1999).

3.5.2 The relationship between pollutants and wind patterns

Wind direction is one of important factors to determine origin of air mass. The frequencies of wind blowing from landfills (%) were calculated based on individual sampling days and the results are shown in Table 2. High percentages of wind flow from landfills were observed in summer at both locations ($p < 0.05$). Spatial variability was also observed, with high frequency of wind flow from landfill at SENT in both seasons. The associations of wind flow from landfills (%) with chemical components are shown in Table S8 (Supplementary Materials) (only significant positive correlations were listed). Significant correlations ($p < 0.01$) were observed between wind frequency from landfills with V (except SENT in summer), Cu and Cl^- ion (except in summer). In addition, NO_3^-, Na^+ and K^+ showed fair correlations with wind frequency. The results indicated significant concentrations of V, Cu, Cl^-, NO_3^-, Na^+ and K^+ were observed when the wind flow from landfill sites. However, no significant associations were observed between DNA damage with wind frequency from landfills.

3.5.3 Correlation between chemical components and DNA damage

The results can be referred to Table 3 for information. Significant positive associations ($p < 0.05$) between chemical components and DNA damage were mainly observed in summer (except Mn, Cd, EC and total PAHs in SENT; Na^+ in WENT; and Sb and Ba in HT during winter). Good correlations were observed for oxidative potential against Zn, Cd, Pb, NH_4^+, K^+ and total PAHs in SENT in summer. DNA damage was positively correlated with NH_4^+ and K^+ in TSW; Pb and NH_4^+ in TKO; and with Zn and Cd in HT. These results are consistent with Shao et al. (2017) that trace elements were associated with particle induced oxidative potential in summer (Shao et al., 2017). However, poor correlations were observed between DNA damage with V, Cu, Cl^-, NO_3^-, and Na^+ in WENT and SENT, which are the species with high correlations to wind frequency flow from landfill sites. The results suggest that these potential landfills orientated species are not associated with oxidative potential responses. In addition, the PLS regression showed no statistically significant differences between physical/chemical characteristics and bioreactivity responses.

3.5.4 Implication of the correlation analysis

The analysis shows significant correlations were observed between wind frequency from landfills with V (except SENT in summer) and Cu (except in summer). Vanadium is a marker for residual oil, exhausts from container ships/landfill machineries (e.g. high emissions from site machineries due to poor maintenance or overloading) that potentially were the sources for these pollutants. Copper (Cu) was identified as a noticeable element in WENT landfill, due to significant amounts of Cu under wind blow from landfill. Both landfills are close to the seashore, high Na^+ and Cl^- concentrations could be potentially due to sea water droplets and marine aerosols. Thus, the high association between Na^+ and Cl^- with wind frequency from landfills was observed in the analysis. However, no significant associations were observed between DNA damage/TD_{50} when increased wind frequency from landfills. In addition, no association were observed between DNA damage with V and Cu, this implied the dominant factor determining the DNA damage was potentially due to other local or regional sources, rather than from a landfill site; although further studies will be necessary in the future (Duffin and Berube, 2006). Significant associations ($p < 0.05$) were mainly observed between DNA damage and heavy metals (Cd and Pb)/PAHs in summer (Liu et al., 2009; Adamson et al., 2000; Xia et al., 2004). Moreover, the DNA damage induced by $PM_{2.5}$ was notably higher in summer than winter. In all of the anthropogenically–derived metals, Cd and Pb are recognized as emitted by high temperature coal and oil combustion processes, such as landfill processing facility (Uberoi et al. and Shadman, 1991). Past studies showed metals are responsible for the generation of ROS, our findings are consistent with previous studies.

This study showed high $PM_{2.5}$ levels during daytime under predominantly wind direction from landfills. Significant associations were observed between DNA damage and heavy metals/PAHs in summer. Emissions from machineries were one of the potential sources in proximity of the landfills. No significant associations were observed between DNA damage when increased wind frequency from landfills which indicated that $PM_{2.5}$ loading from other sources (e.g. regional sources) was an important contributing factor for DNA damage. However, limitations occurred such as the sampling frequency was only in every three days for a period of ~ 4 months in the two seasons and insufficient information about the landfills processing facilities could hinder the evaluation of air pollutants levels.

Acknowledgments

This study was supported by the Research Grants Council of the Hong Kong Special Administrative Region China (Project No. CUHK 412612).

References

Adamson, I., Prieditis, H., Hedgecock, C., Vincent, R., 2000. Zinc is the toxic factor in the lung response to an atmospheric particulate sample. *Toxicol. Appl. Pharmacol.* 166, 111-119.

Berube, K. A., Jones, T. P., Williamson, B., Winters, C., Morgan, A. J., Richards, R., 1999. Physicochemical characterisation of diesel exhaust particles: Factors for assessing biological activity. *Atmos. Environ.* 33, 1599-1614.

Bitterle, E., Karg, E., Schroeppel, A., Kreyling, W., Tippe, A., Ferron, G., Schmid, O., Heyder, J., Maier, K., Hofer, T., 2006. Dose-controlled exposure of A549 epithelial cells at the air–liquid interface to airborne ultrafine carbonaceous particles. *Chemosphere* 65, 1784-1790.

Cao, J., Lee, S., Ho, K., Zou, S., Fung, K., Li, Y., Watson, J. G., Chow, J. C., 2004. Spatial and seasonal variations of atmospheric organic carbon and elemental carbon in Pearl River Delta Region, China. *Atmos. Environ.* 38, 4447-4456.

Charrier, J. G., McFall, A. S., Richards-Henderson, N. K., Anastasio, C., 2014. Hydrogen peroxide formation in a surrogate lung fluid by transition metals and quinones present in particulate matter. *Environ. Sci. Technol.* 48, 7010-7017.

Costa, D. L., Dreher, K. L., 1997. Bioavailable transition metals in particulate matter mediate cardiopulmonary injury in healthy and compromised animal models. *Environ. Health Perspect.* 105, 1053.

Deed, C., 2004. Monitoring of particulate matter in ambient air around waste facilities, Technical Guidance Document (Monitoring) M17, Publ, Environment Agency, Bristol, ISBN, 1, 322610.

Donaldson, K., Beswick, P. H., Gilmour, P. S., 1996. Free radical activity associated with the surface of particles: a unifying factor in determining biological activity?. *Toxicol. Lett.* 88, 293-298.

Duffin, R., Berube, K., 2006. British Association for Lung Research-Summer 2005 Meeting Summary-Abstracts. *Exp. Lung Res.* 32, 119-+.

Gilmour, P., Beswick, P., Donaldson, K., 1994. Effects of asbestos and a range of respirable industrial fibres on super-coiled plasmid DNA. *Respiratory Med.* 88, 812-813.

HKEPD, 2015. *Monitoring of Solid Waste in Hong Kong, Waste Statistics for 2015*. The Government of the Hong Kong Special Administrative Region, Hong Kong Environmental Protection Department (HKEPD): (accessed 18.10.18).

HKEPD, 2016. *South East New Territories Landfill to receive only construction waste from January 6*; The Government of the Hong Kong Special Administrative Region, Hong Kong Environmental Protection Department (HKEPD): (accessed 18.10.18).

Ho, K., Lee, S., Chan, C. K., Jimmy, C. Y., Chow, J. C., Yao, X., 2003. Characterization of chemical species in PM 2.5 and PM 10 aerosols in Hong Kong. *Atmos. Environ.* 37, 31-39.

Hou, X., Chan, C.K., Dong, G.H., Yim, S.H.L., 2018. Impacts of transboundary air pollution and local emissions on PM2. 5 pollution in the Pearl River Delta region of China and the public health, and the policy implications. *Environ. Res. Lett.* 14, 034005.

Jarup, L., Briggs, D., De Hoogh, C., Morris, S., Hurt, C., Lewin, A., Maitland, I., Richardson, S., Wakefield, J., Elliott, P., 2012. Cancer risks in populations living near landfill sites in Great Britain. *Br. J. Cancer* 86, 1732.

Jones, T., Moreno, T., BéruBé, K., Richards, R., 2006. The physicochemical characterisation of microscopic airborne particles in south Wales: a review of the locations and methodologies. *Sci. Total Environ.* 360, 43-59.

Koshy, L., Paris, E., Ling, S., Jones, T., BéruBé, K., 2007. Bioreactivity of leachate from municipal solid waste landfills—assessment of toxicity. *Sci. Total Environ. 384*, 171-181.

Koshy, L., Jones, T., BéruBé, K., 2009. Characterization and bioreactivity of respirable airborne particles from a municipal landfill. *Biomarkers* 14, 49-53.

Leung, P., Wan, H., Billah, M., Cao, J., Ho, K., Wong, C. K., 2014. Chemical and biological characterization of air particulate matter 2.5, collected from five cities in China. *Environ. Pollut.* 194, 188-195.

Lingard, J., Tomlin, A., Clarke, A., Healey, K., Hay, A., Wild, C., Routledge, M., 2005. A study of trace metal concentration of urban airborne particulate matter and its role in free radical activity as measured by plasmid strand break assay. *Atmos. Environ.* 39, 2377-2384.

Liu, J., Qu, W., Kadiiska, M. B., 2009. Role of oxidative stress in cadmium toxicity and carcinogenesis. *Toxicol. Appl. Pharmacol.* 238, 209-214.

Luo, M., Hou, X., Gu, Y., Lau, N.-C., Yim, S.H.-L., 2018. Trans-boundary air pollution in a city under various atmospheric conditions. *Sci. Total Environ.* 618, 132-141.

Macklin, Y., Kibble, A., Pollitt, F., 2011. Impact on health of emissions from landfill sites, Advice from the Health Protection Agency.

Miller, M.R., Shaw, C.A., Langrish, J.P., 2012. From particles to patients: oxidative stress and the cardiovascular effects of air pollution. *Future Cardiol.* 8, 577-602.

Moreno, T., Merolla, L., Gibbons, W., Greenwell, L., Jones, T., Richards, R., 2004. Variations in the source, metal content and bioreactivity of technogenic aerosols: a case study from Port Talbot, Wales, UK. *Sci. Total Environ.* 333, 59-73.

Okuda, T., Okamoto, K., Tanaka, S., Shen, Z., Han, Y., Huo, Z., 2010. Measurement and source identification of polycyclic aromatic hydrocarbons (PAHs) in the aerosol in Xi'an, China, by using automated column chromatography and applying positive matrix factorization (PMF). *Sci. Total Environ.* 408, 1909-1914.

Palmer, S. R., Dunstan, F. D., Fielder, H., Fone, D. L., Higgs, G., Senior, M. L., 2005. Risk of congenital anomalies after the opening of landfill sites. *Environ. Health Perspect.* 113, 1362.

Pope III, C. A., Thun, M. J., Namboodiri, M M., Dockery, D. W., Evans, J. S., Speizer, F. E., 1995. Heath Jr, C. W. Particulate air pollution as a predictor of mortality in a prospective study of US adults. *Am. J. Respiratory Critical Care Med.* 151, 669-674.

Rogge, W. F., Mazurek, M. A., Hildemann, L. M., Cass, G. R., Simoneit, B. R., 1993. Quantification of urban organic aerosols at a molecular level: identification, abundance and seasonal variation. *Atmos. Environ. Part A. General Topics* 27, 1309-1330.

Shao, L., Shen, R., Wang, J., Wang, Z., Tang, U., Yang, S., 2013. A toxicological study of inhalable particulates by plasmid DNA assay: A case study from Macao. *Sci. China Earth Sciences* 56, 1037-1043.

Shao, L., Hu, Y., Shen, R., Schäfer, K., Wang, J., Wang, J., Schnelle-Kreis, J., Zimmermann, R., BéruBé, K., Suppan, P., 2017. Seasonal variation of particle-induced oxidative potential of airborne particulate matter in Beijing. *Sci. Total Environ.* 579, 1152-1160.

Sillanpää, M., Frey, A., Hillamo, R., Pennanen, A., Salonen, R., 2005. Organic, elemental and inorganic carbon in particulate matter of six urban environments in Europe. *Atmos. Chem. Phys.* 5, 2869-2879.

Stone, V., Shaw, J., Brown, D., MacNee, W., Faux, S., Donaldson, K., 1998. The role of oxidative stress in the prolonged inhibitory effect of ultrafine carbon black on epithelial cell function. *Toxicol. In Vitro* 12, 649-659.

Tong, C.H.M., Yim, S.H.L., Rothenberg, D., Wang, C., Lin, C.-Y., Chen, Y.D., Lau, N.C., 2018. Assessing the impacts of seasonal and vertical atmospheric conditions on air quality over the Pearl River Delta region. *Atmos. Environ.* 180, 69-78.

Uberoi, M., Shadman, F., 1991. High-temperature removal of cadmium compounds using solid sorbents. *Environ. Sci. Technol.* 25, 1285-1289.

U.S. EPA, 2013. *Municipal Solid Waste in the United States*; EPA: Washington, DC, 2013. United States Environmental Protection Agency (US EPA): https://archive.epa.gov/epawaste/nonhaz/municipal/web/html/: (accessed 18.10.18).

Wang, G., Wang, H., Yu, Y., Gao, S., Feng, J., Gao, S., Wang, L., 2003. Chemical characterization of water-soluble components of PM 10 and PM 2.5 atmospheric aerosols in five locations of Nanjing, China. *Atmos. Environ.* 37, 2893-2902.

Wang, T., Guo, H., Blake, D., Kwok, Y., Simpson, I., Li, Y., 2005. Measurements of trace gases in the inflow of South China Sea background air and outflow of regional pollution at Tai O, Southern China. *J. Atmos. Chem.* 52, 295.

Xia, T., Korge, P., Weiss, J. N., Li, N., Venkatesen, M. I., Sioutas, C., Nel, A., 2004. Quinones and aromatic chemical compounds in particulate matter induce mitochondrial dysfunction: implications for ultrafine particle toxicity. *Environ. Health Perspect.* 112, 1347.

Xiao, Z., Shao, L., Zhang, N., Wang, J., Chuang, H.-C., Deng, Z., Wang, Z., BéruBé, K., 2014. A toxicological study of inhalable particulates in an industrial region of Lanzhou City, northwestern China: Results from plasmid scission assay. *Aeolian Res.* 14, 25-34.

Xu, H., Ho, S. S. H., Gao, M., Cao, J., Guinot, B., Ho, K. F., Long, X., Wang, J., Shen, Z., Liu, S., 2016. Microscale spatial distribution and health assessment of PM 2.5-bound polycyclic aromatic hydrocarbons (PAHs) at nine communities in Xi'an, China. *Environ. Pollut.* 218, 1065-1073.

Yim, S., Fung, J., Lau, A., 2009. Mesoscale simulation of year-to-year variation of wind power potential over southern China. *Energies* 2, 340-361.

Yim, S., Hou, X., Guo, J., Yang, Y., 2019. Contribution of local emissions and transboundary air pollution to air quality in Hong Kong during El Niño-Southern Oscillation and heatwaves. *Atmos. Res.* 218, 50-58.

Yim, S.H., Fung, J.C., Lau, A.K., 2010. Use of high-resolution MM5/CALMET/CALPUFF system: SO2 apportionment to air quality in Hong Kong. *Atmos. Environ.* 44, 4850-4858.

Yuan, Z., Yu, J., Lau, A., Louie, P., Fung, J., 2006. Application of positive matrix factorization in estimating aerosol secondary organic carbon in Hong Kong and its relationship with secondary sulfate. *Atmos. Chem. Phys.* 6, 25-34.

Yue, W., Li, X., Liu, J., Li, Y., Yu, X., Deng, B., Wan, T., Zhang, G., Huang, Y., He, W., 2006. Characterization of PM 2.5 in the ambient air of Shanghai city by analyzing individual particles. *Sci. Total Environ.* 368, 916-925.

Zhang, L., Chen, R., Lv, J., 2016. Spatial and Seasonal Variations of Polycyclic Aromatic Hydrocarbons (PAHs) in Ambient Particulate Matter (PM10). *Bull. Environ. Contam. Toxicol.* 96, 827-832.

Zhuang, H., Chan, C. K., Fang, M., Wexler, A. S., 1999. Formation of nitrate and non-sea-salt sulfate on coarse particles. *Atmos. Environ.* 33, 4223-4233.

List of Tables

List of Figures and Figure Legends

Figure 3 Hourly average of $PM_{2.5}$ concentration at SENT in a) winter and b) summer.

Figure 4 Scanning electron microscope images reveal morphologies of $PM_{2.5}$ samples near the landfill sites.

Table 1 The average DNA damage induced by $PM_{2.5}$ collected from five sampling locations in winter and summer.

	Winter		Summer	
Sampling location	TD_{50} *(μg ml^{-1})	DNA damage** (%)	TD_{50} (μg ml^{-1})	DNA damage (%)
WENT	227.5±294.0	39.1±16.3	41.8±16.1	70.2±23.2
SENT	118.6±82.8	46.0±20.3	48.0±26.4	67.2±24.9
TSW	95.5±48.8	39.1±21.7	51.3±22.3	60.7±25.5
TKO	61.3±39.7	62.1±19.1	54.5±14.1	48.6±11.4
HT	102.8±82.5	43.0±18.2	63.3± 69.0	64.4±25.4

*The toxic dosage of particulate matter causing DNA damage (TD_{50}) denotes the toxic dosage of $PM_{2.5}$ causing 50% DNA damage.

**The amount of damage to the plasmid DNA induced by $PM_{2.5}$ under 100 μg ml^{-1} dosage.

Table 2 The average frequencies (%) of wind blowing from landfills in winter and summer.

	Winter*		Summer	
Sampling location	Mean	Range	Mean	Range
WENT	30.7±13.9	4.3-51.8	43.3±19.1	7.1-71.8
SENT	60.8±17.7	11.2-84.0	66.1±18.7	18.6-84.8

*The frequencies (%) were based on individual sampling days.

Table 3 Spearman's rank correlation coefficients (r) between DNA damage and $PM_{2.5}$ components.

	WENT		SENT		TSW		TKO		HT	
Components	Winter	Summer	Winter	Summer	Winter	Summer	Winter	Summer	Winter	Summer
Mg	0.26	-0.16	-0.05	-0.61	-0.31	-0.32	-0.47	-0.84	-0.12	-0.68
Ca	-0.57	-0.39	0.25	-0.50	-0.15	-0.64	-0.77	-0.02	-0.02	-0.31
V	-0.06	-0.09	-0.05	-0.76	0.12	-0.27	-0.63	-0.49	-0.05	-0.30
Cr	-0.01	0.03	-0.32	-0.51	-0.42	-0.23	-0.62	-0.51	0.22	-0.53
Mn	0.08	0.21	0.62	0.05	0.17	0.09	-0.73	-0.21	-0.12	0.04
Fe	-0.14	0.19	-0.02	-0.70	0.63	-0.13	-0.13	-0.46	-0.17	-0.03
Ni	0.04	0.09	-0.55	-0.80	0.46	-0.40	-0.02	-0.47	-0.34	-0.41
Cu	0.01	0.01	-0.30	-0.58	-0.42	0.13	0.45	0.05	-0.01	-0.52
Zn	-0.10	0.34	-0.05	**0.77^{++}**	0.25	0.35	0.30	0.54	-0.05	0.72
As	0.07	0.44	0.47	0.24	0.44	0.45	0.07	0.39	0.00	0.24
Cd	-0.13	0.42	**0.67^{+}**	**0.82^{++}**	-0.32	0.62	0.32	0.46	0.31	**0.71^{++}**
Sb	-0.04	-0.10	0.32	-0.01	-0.05	0.18	0.30	-0.22	0.67	-0.48
Ba	-0.29	-0.33	0.35	0.12	-0.76	-0.33	-0.07	-0.10	0.60	-0.10
Pb	-0.13	0.36	0.22	**0.79^{++}**	0.36	0.35	0.37	**0.67^{+}**	0.13	0.46
OC	-0.53	0.52	0.23	0.56	-0.08	0.47	0.38	0.58	0.21	0.27
EC	-0.51	0.36	**0.83^{++}**	0.18	-0.14	0.34	0.48	0.36	-0.26	0.10
Cl^-	0.61	-0.41	-0.28	-0.80	-0.03	-0.59	0.40	-0.56	0.05	-0.72
NO_3^-	0.07	-0.48	-0.55	-0.51	0.05	-0.06	0.10	-0.30	0.20	-0.50
SO_4^{2-}	0.10	-0.26	0.10	-0.32	-0.03	-0.37	-0.55	-0.15	-0.08	-0.09
Na^+	0.62	-0.10	-0.35	-0.93	0.12	-0.37	-0.20	-0.80	0.09	-0.69
NH_4^+	0.22	0.16	-0.18	**0.73^{+}**	-0.08	**0.66^{+}**	-0.37	**0.62^{+}**	-0.05	0.52
K^+	-0.05	-0.09	0.53	**0.90^{+}**	0.58	**0.90^{+}**	0.50	0.15	-0.25	0.43
ACE	0.13	-0.19	-0.80	-0.31	0.51	0.16	-0.10	-0.41	0.36	-0.35
FLU	0.05	0.42	-0.03	0.16	0.37	0.42	0.03	-0.05	0.46	-0.68
PHE	-0.78	0.27	0.62	-0.02	0.41	0.60	0.30	0.22	-0.26	-0.16
ANT	-0.85	0.24	0.47	-0.36	0.63	0.43	0.00	0.01	-0.24	-0.13
FLT	-0.72	0.31	0.65	**0.89^{++}**	-0.22	0.48	0.45	**0.79^{++}**	-0.28	0.52
PYR	-0.78	0.33	**0.70^{+}**	**0.85^{++}**	0.19	**0.77^{++}**	0.32	**0.76^{++}**	-0.27	0.36
BaA	-0.34	0.41	0.50	**0.67^{+}**	0.48	0.59	-0.12	**0.80^{++}**	-0.38	0.53
CHR	-0.34	0.18	**0.70^{+}**	**0.65^{+}**	0.31	0.59	0.15	**0.79^{++}**	-0.30	0.46
BbF	-0.56	0.23	**0.67^{+}**	**0.78^{++}**	0.58	0.48	0.08	**0.80^{++}**	-0.33	0.49
BkF	-0.47	0.20	**0.75^{+}**	**0.71^{+}**	0.41	0.50	0.18	**0.72^{+}**	-0.42	**0.59^{+}**
BaF	-0.58	0.21	**0.83^{++}**	**0.76^{++}**	0.56	0.51	0.03	**0.87^{++}**	-0.33	0.44

BeP	-0.67	0.27	**0.80**$^{++}$	**0.77**$^{++}$	0.58	0.45	0.10	**0.76**$^{++}$	-0.35	0.53
BaP	-0.67	0.40	**0.85**$^{++}$	**0.71**$^{+}$	0.32	0.50	0.15	**0.72**$^{+}$	-0.20	0.48
PER	-0.58	0.44	0.60	0.56	0.53	0.43	-0.48	**0.69**$^{+}$	-0.05	**0.60**$^{+}$
INP	-0.67	0.29	**0.85**$^{++}$	**0.69**$^{+}$	0.58	0.46	0.25	**0.61**$^{+}$	-0.31	0.39
BghiP	-0.67	0.35	**0.82**$^{++}$	**0.67**$^{+}$	0.58	0.42	-0.03	0.58	-0.17	0.41
DahA	-0.67	0.27	**0.83**$^{++}$	**0.65**$^{+}$	0.46	0.43	0.21	0.49	-0.34	0.44
COR	-0.65	0.36	0.58	**0.85**$^{++}$	0.58	0.43	-0.28	**0.70**$^{+}$	-0.02	0.25
Total PAHs	-0.67	0.29	**0.72**$^{+}$	**0.64**$^{+}$	0.58	0.45	0.03	**0.78**$^{++}$	-0.24	0.36

+, positive correlation, $p < 0.05$.

++, positive correlation, $p < 0.01$.

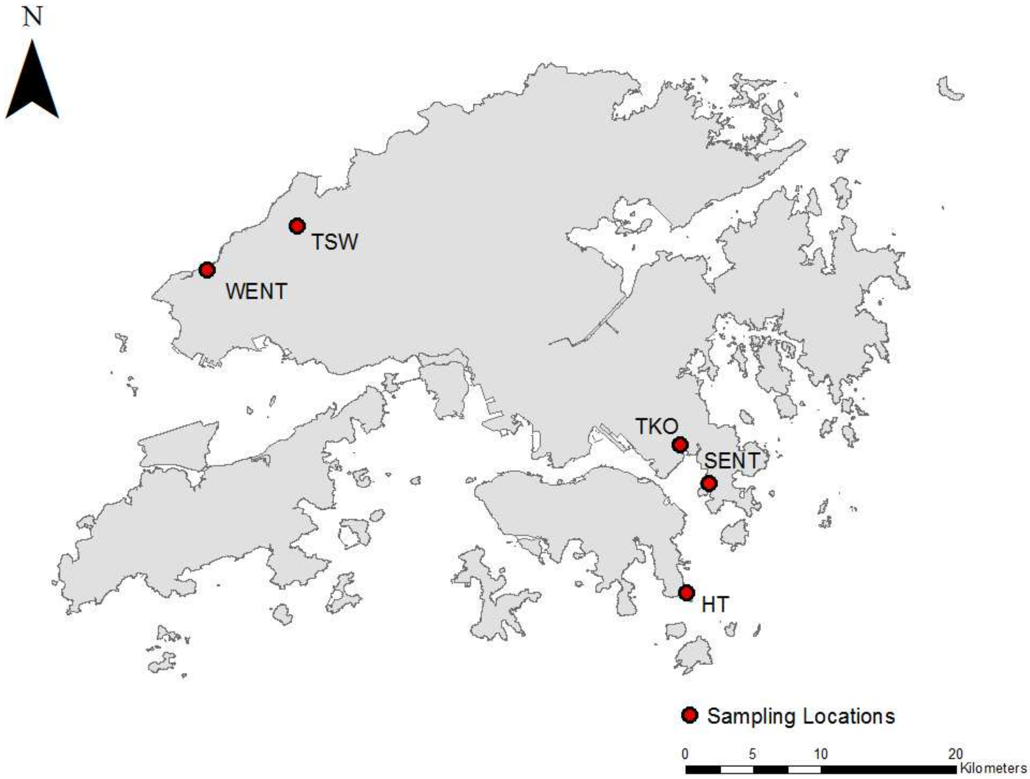

Figure 1 Locations of sampling sites.

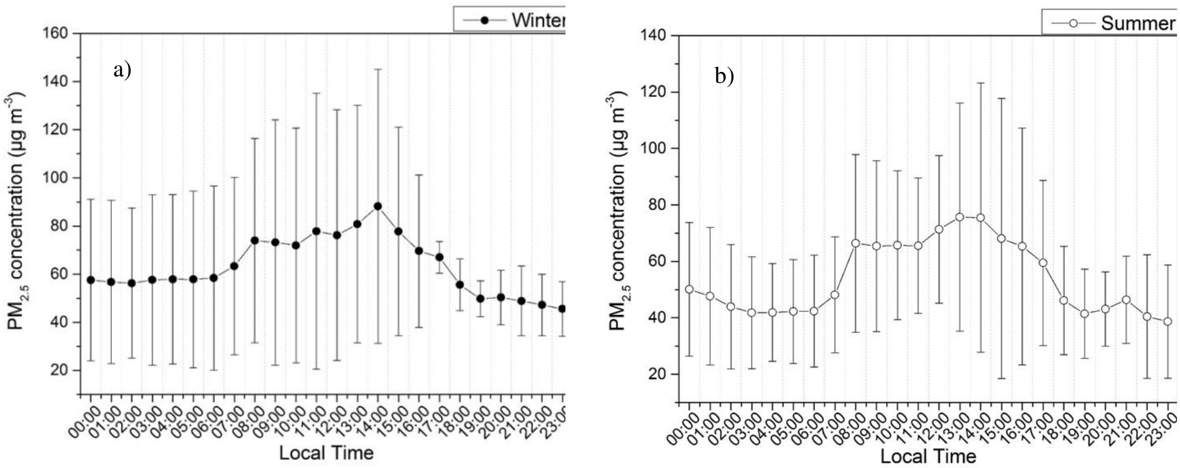

Figure 2 Hourly average $PM_{2.5}$ concentration at WENT in a) winter and b) summer.

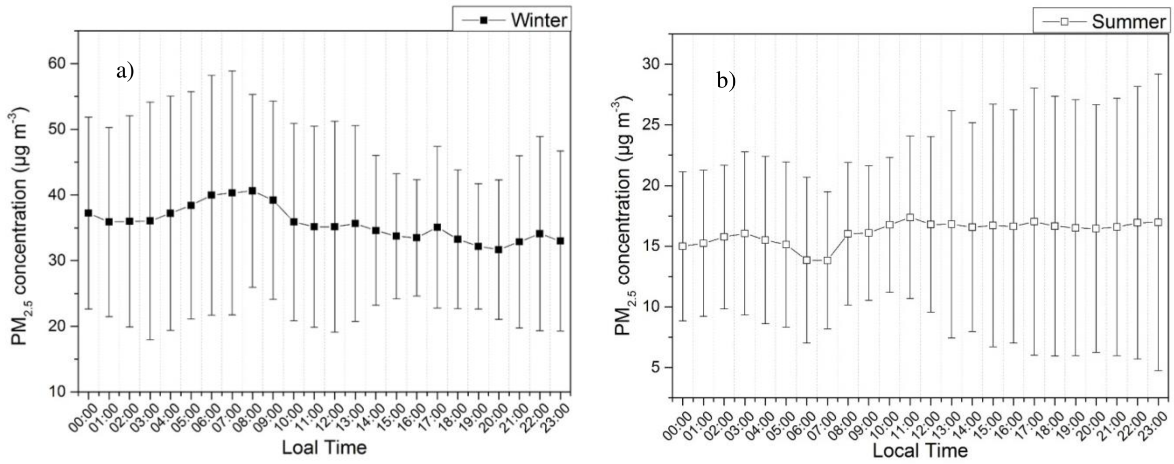

Figure 3 Hourly average of $PM_{2.5}$ concentration at SENT in a) winter and b) summer.

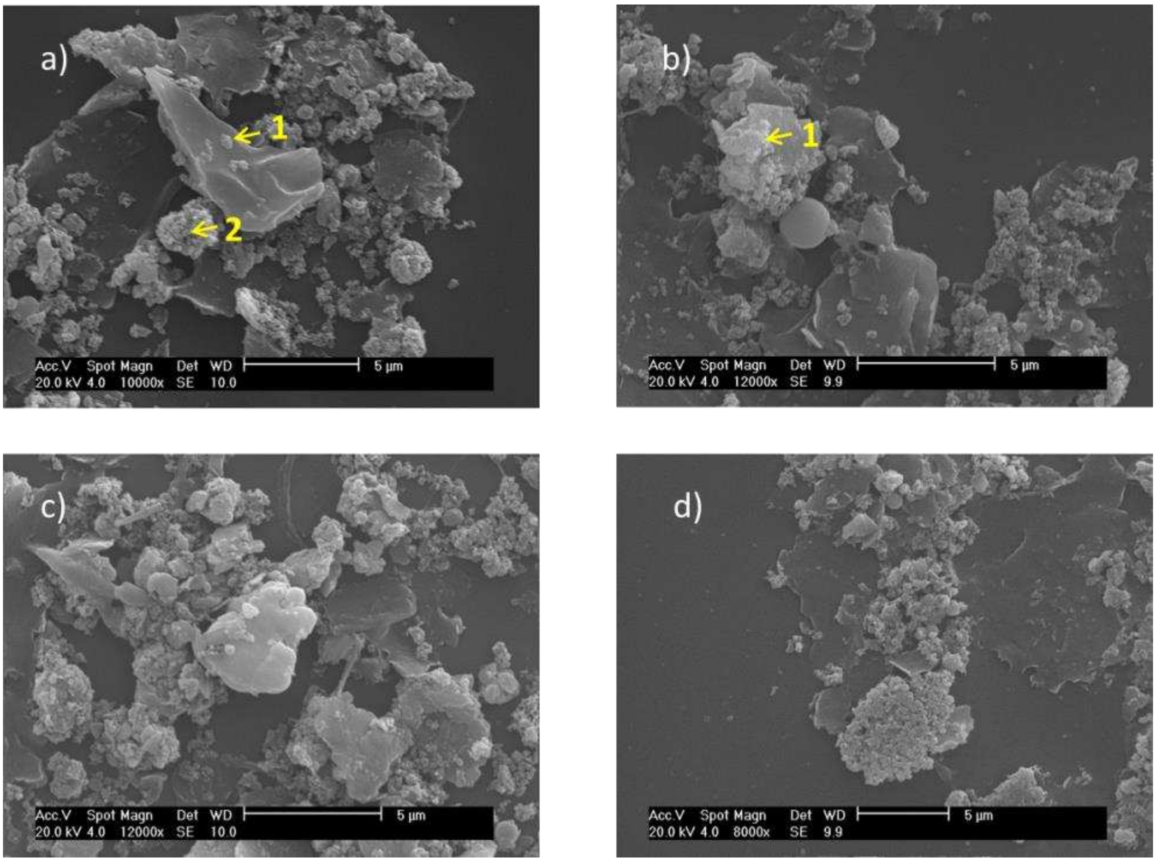

Figure 4 Scanning electron microscope images reveal morphologies of $PM_{2.5}$ samples near the landfill sites.